# Transport properties of single-crystalline n-type semiconducting PbTe nanowires



2009 Nanotechnology 20 415204

(http://iopscience.iop.org/0957-4484/20/41/415204)

Nanotechnology **20** (2009) 415204 (4pp) doi:10.1088/0957-4484/20/41/415204

# Transport properties of single-crystalline n-type semiconducting PbTe nanowires

**So Young Jang[1,4], Han Sung Kim[1], Jeunghee Park[1,5], Minkyung Jung[2], Jinhee Kim[2], Seung Hyun Lee[3,4], Jong Wook Roh[3] and Wooyoung Lee[3,5]**

[1] Department of Chemistry, Korea University, Jochiwon 339-700, Korea
[2] Korea Research Institute of Standard and Science, Daejeon 305-600, Korea
[3] Nanomedical National Core Research Center and Department of Materials Science and Engineering, Yonsei University, Seoul 120-749, Korea

E-mail: parkjh@korea.ac.kr and wooyoung@yonsei.ac.kr

Received 4 June 2009, in final form 25 August 2009
Published 16 September 2009
Online at stacks.iop.org/Nano/20/415204

**Abstract**
Single-crystalline PbTe nanowires were synthesized using the chemical vapor transport method. They consisted of rock-salt structure PbTe nanocrystals uniformly grown in the [100] direction. We fabricated field-effect transistors using a single PbTe nanowire, providing evidence for its intrinsic n-type semiconductor characteristics. The values of the carrier mobility and concentration were estimated to be 0.83 $cm^2\ V^{-1}\ s^{-1}$ and $8.8 \times 10^{17}\ cm^{-3}$, respectively. The Seebeck coefficients ($-72\ \mu V\ K^{-1}$) of individual nanowires were measured to show their n-type carrier-dominated thermoelectric transport properties.

S Supplementary data are available from stacks.iop.org/Nano/20/415204

(Some figures in this article are in colour only in the electronic version)

## 1. Introduction

Since the discovery of carbon nanotubes (CNTs), a tremendous amount of research has been conducted on the synthesis and utilization of one-dimensional (1D) nanostructures as well-defined building blocks for future nanodevices using 'bottom up' approaches [1]. As one of the important IV–VI semiconductor materials, the rock-salt (face-centered cubic) structured lead telluride (PbTe) nanostructure has been the object of particular attention, because of its narrow band gap of 0.31 eV (in the bulk at room temperature) and strong quantum confinement effect owing to its large Bohr radius (about $r_B = 46$ nm). The synthesis of PbTe nanocrystals [2–4], nanorods [5], nanotubes [6], dendrites [7], and nanowires [8–14], has been reported by a number of research groups. In particular, the PbTe nanowires (NWs) are of great interest for the construction of high-performance thermoelectric devices [9–12]. Yang and co-workers measured the thermal conductivity of single p-type semiconducting PbTe NWs to show the effects of phonon confinement as the diameter of the nanowire decreases [9]. Tai *et al* [10, 11] and Yan *et al* [12] reported the hydrothermal synthesis of p-type PbTe NWs and the larger thermoelectric power (positive Seebeck coefficient) of a nanowire network film compared to that of the bulk. Nevertheless, no studies have been carried out on the electric or thermoelectric properties of n-type PbTe NWs. In the present study, we report the synthesis of single-crystalline PbTe NWs using the chemical vapor transport method, and their unique electric/thermoelectric properties. We fabricated field-effect transistors (FETs) using single PbTe NWs, proving it to be an intrinsically n-type semiconductor. The Seebeck coefficient of single PbTe NW was first measured to give constant evidence for such n-type semiconducting behaviors.

## 2. Experimental details

For the synthesis of PbTe NWs, mixed lead (II) chloride ($PbCl_2$, 99.999%, Aldrich) and tellurium (Te, 99.8%, Aldrich) powders with 1:1 mol ratio were placed inside a quartz tube reactor. A silicon substrate on which 3 nm thick Au film was deposited was positioned at a distance of 10 cm from

[4] These authors contributed equally to this work.
[5] Authors to whom any correspondence should be addressed.

 

the PbTe source. As the source was allowed to evaporate at 1100 °C for 2 h under an argon flow (300 sccm), the NWs grew on the substrate at 900 °C. The products were analyzed by scanning electron microscopy (SEM, Hitachi S-4700), field-emission transmission electron microscopy (TEM, FEI TECNAI $G^2$ 200 kV and Jeol JEM 2100F), high-voltage TEM (HVEM, Jeol JEM ARM 1300S, 1.25 MV), electron diffraction (ED), and energy-dispersive x-ray fluorescence spectroscopy (EDX). High-resolution x-ray diffraction (XRD) patterns were obtained using the 8C2 and 3C2 beam line of the Pohang Light Source (PLS) with monochromatic radiation ($\lambda = 1.545\,20$ Å). X-ray photoelectron spectroscopy (XPS) was carried out using the 8A1 beam line of the PLS and a laboratory-based spectrometer (VG Scientifics ESCALAB 250) using a photon energy of 1486.6 eV (Al K$\alpha$).

## 3. Results and discussion

Figure 1(a) shows an SEM image of PbTe NWs grown on a Si substrate. The growth mechanism follows the vapor–liquid–solid (VLS) mechanism using 3 nm-thick-film Au catalysts. The TEM image reveals that their surface is smooth and their diameter is in the range of 100–150 nm, with an average value of 130 nm (figures 1(b) and (c)). Figure 1(d) shows the lattice-resolved TEM image for the selected NWs shown in figure 1(c), revealing that they are perfect single-crystalline nanowires. The (200) fringes are separated by a distance of 3.2 Å, which is equal to that of rock-salt (cubic) PbTe crystal ($a = 6.454$ Å; JCPDS Card No. 78-1905). The corresponding selected-area electron diffraction (SAED) pattern, measured at the [001] zone axis, confirms that the single-crystalline nanowires grew in the [100] direction (inset). The XRD pattern of the PbTe NWs confirms the formation of pure PbTe phase, without any other phases (figure 1(e)). The figure shows all of the peaks that would be expected for rock-salt PbTe (JCPDS No. 78-1905; $a = 6.454$ Å). The EDX data were obtained for a number (>30) of the NWs, showing a ratio of Pb/Te $\approx 1$, without any doping impurities (supporting information, figure S1 available at stacks.iop.org/Nano/20/415204). The XPS data confirm the same ratio (supporting information, figure S2 available at stacks.iop.org/Nano/20/415204).

We fabricated the PbTe NW FET electrodes by the following procedure. The nanowires, dispersed in isopropyl alcohol (IPA), were dropped onto an Si substrate with a 300 nm thick thermally grown $SiO_2$ layer on which alignment marks had been made. The spatial position and orientation of the nanowire were recorded by digitizing the coordinates from the optical microscopy images. The electrical leads were defined on the selected nanowire using electron beam lithography. A plasma etching system was used to remove the oxide layer from the outer surface of the nanowires. For the ohmic contact, Cr (5 nm)/Au (130 nm) films were deposited on the contact area by electron beam evaporation. The etching and deposition of the electrodes were carried out *in situ* without breaking the vacuum, in order to prevent the further formation of the oxide layer. The underlying Si substrate was used as the back gate by forming an ohmic contact with an Al electrode.

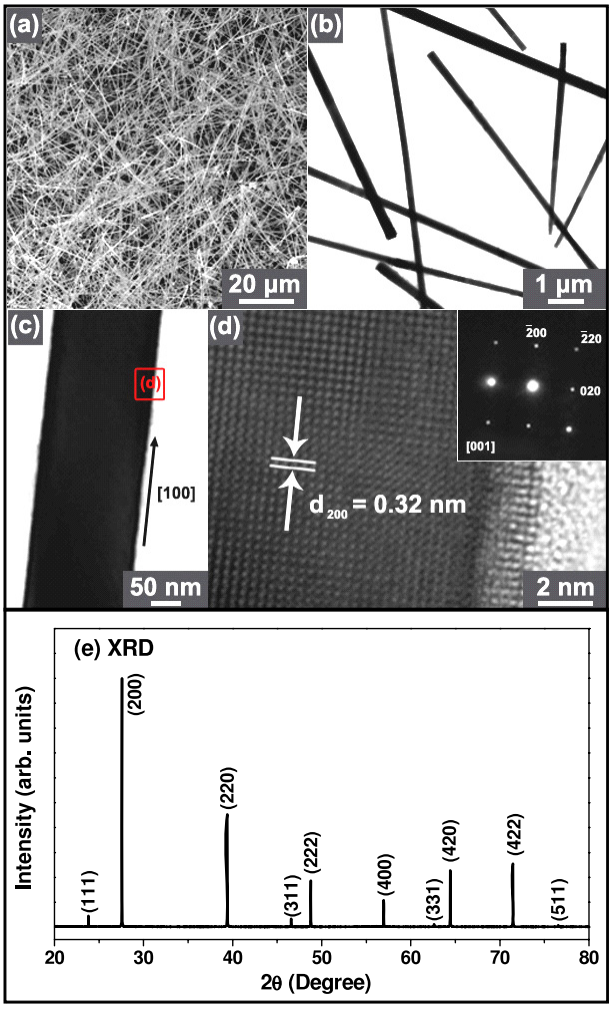


**Figure 1.** (a) SEM image showing the high-density PbTe NWs. (b) TEM image revealing the straight nanowire morphology. (c) TEM image of representative PbTe NW, and (d) its lattice-resolved TEM image, revealing the highly crystalline cubic (200) PbTe planes. The SAED pattern (at the [001] zone axis) confirms that the single-crystalline nanowires grew in the [100] direction (inset). (e) XRD pattern of the PbTe NWs.

Using ten different PbTe NW FET devices, we measured the reproducible source–drain current ($I$) versus voltage ($V_{SD}$) curves at different gate voltages ($V_G = -10$–10 V), as shown in figure 2. The SEM image of the NW FET is shown in the inset. The two-terminal $I$–$V_{SD}$ curves exhibit a nearly linear response at zero bias and, thus, the contacts behave, in practical terms, as ohmic ones. For a given $V_{SD}$, $I$ increases slightly with increasing positive $V_G$, indicating the n-type semiconductor characteristics of the PbTe NWs. From the linear region of the $I$–$V_G$ curve at a fixed $V_{SD} = 1$ V, the transconductance ($g_m = dI/dV_G$) can be extrapolated (figure 2(b)). The hollow circles and the line represent the data points and linear fit, respectively. The channel mobility of the device, $\mu_h$, was estimated to be 0.83 $cm^2\ V^{-1}\ s^{-1}$, using the equation, $\mu_h = g_m \frac{L^2}{CV_{SD}}$, where $L$ is the channel length (=1.8 $\mu$m) of the NW FET and $C$ is the capacitance of the nanowire [15]. The capacitance of the nanowire, $C$, is given by $c = \frac{2\pi\varepsilon\varepsilon_0 L}{\ln(2h/r)}$, where $\varepsilon$ is the relative dielectric constant of $SiO_2$ (=3.9), $h$ is the thickness

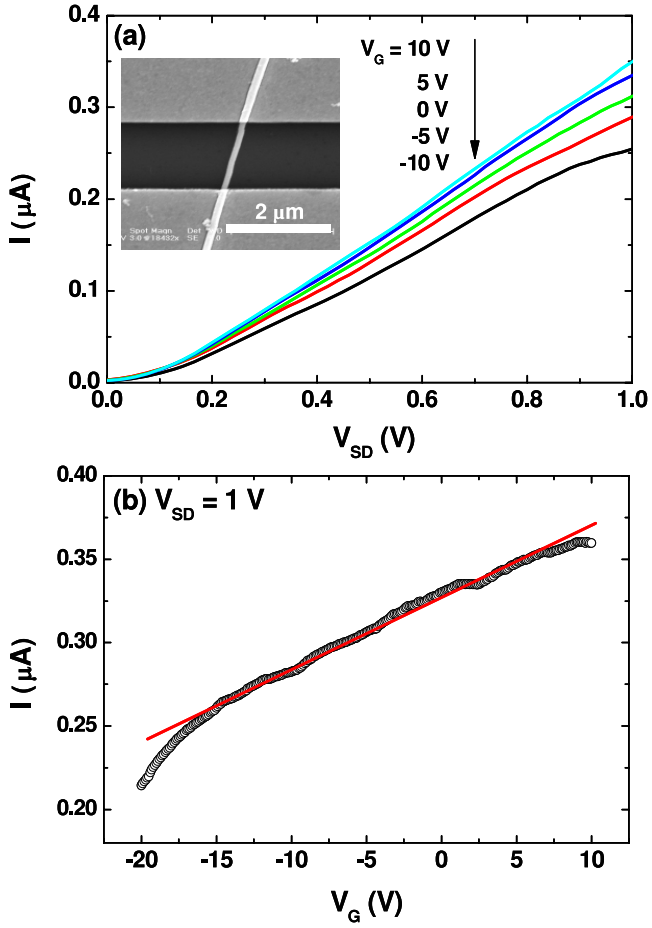


**Figure 2.** Current versus source–drain ($I$–$V_{SD}$) curves at different gate voltages ($V_G = -10$–10 V) of a FET made of a single PbTe NW. Inset corresponds to the SEM image of the PbTe NW FET. (b) $I$–$V_G$ data (hollow circles) at $V_{SD} = 1$ V and their linear fit (line).

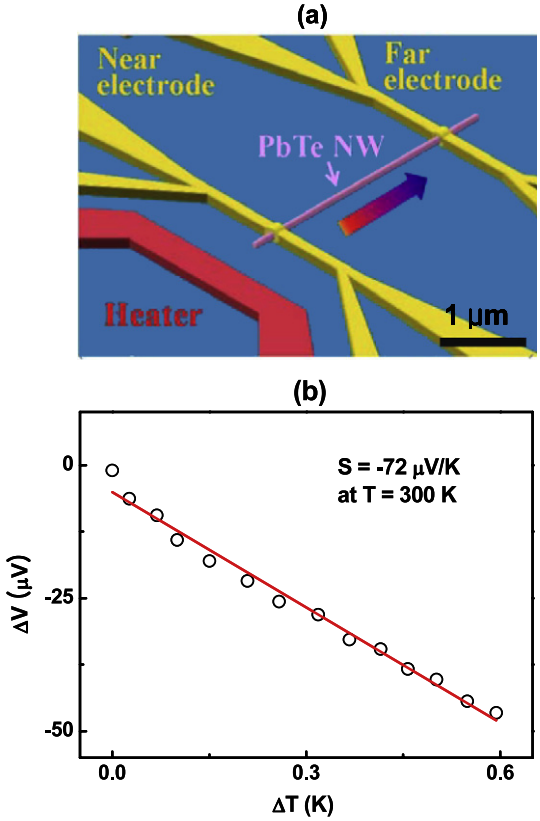


**Figure 3.** (a) Schematic diagram of PbTe NW thermoelectric device. (b) Thermoelectric voltage ($\Delta V$) versus temperature difference ($\Delta T$), providing $S = -72\ \mu$V K$^{-1}$ at room temperature.

of the silicon oxide layer (=300 nm), and $r$ is the radius of the nanowire (60 nm). The $I$–$V_G$ data yield a resistivity of 2.3 Ω cm. By using the channel length in the 1D electrical transport model, an electrical conductivity $\sigma = 0.44$ S m$^{-1}$ can be obtained. The carrier density ($n$) is defined by $n = \frac{\sigma}{e\mu}$, giving a value of $n = 8.8 \times 10^{17}$ cm$^{-3}$. The mobility of the present NW is close to that (0.71 cm$^2$ V$^{-1}$ s$^{-1}$) of p-type PbTe NWs ($n = 8.4 \times 10^{19}$ cm$^3$) measured by Fardy *et al* [9].

In order to investigate the thermoelectric properties of PbTe NWs, the Seebeck coefficient ($S$) was measured using another PbTe NW (radius = 68 nm). A schematic diagram of a representative device is shown in figure 3(a). A combination of electron beam lithography and a lift-off process was utilized to fabricate inner micron-scaled Cr (5 nm)/Au (130 nm) electrodes with resistances of $R_n$ (resistance of near electrode) and $R_f$ (resistance of far electrode) and a microheater connecting the PbTe NW on the grid of points. A bias voltage was applied to the heater line in order to produce joule heating and to raise the temperature locally around the adjacent contact area. The heat generated by the local heater was designed to propagate initially through the 0.5 $\mu$m-thick $SiO_2$ layer, providing a temperature gradient across the PbTe NW and the surface of the $SiO_2$ layer to which it is thermally anchored due to its low thermal conductivity (∼0.5 W m$^{-1}$ K$^{-1}$). The temperature of the nanowire–electrode junctions was monitored by measuring the variations of the $R_n$ and $R_f$ values of the electrodes using the four-probe method. The resultant temperature gradient across the nanowire was found to be 0.1–0.2 K $\mu$m$^{-1}$, while the typical power consumption in the microheater was less than 100 $\mu$W. The thermoelectric voltages across the PbTe NW can be readily measured via the electrode contacts with a high-input resistance nanovoltmeter.

The heater current ($I_h$) applied to the heater causes a temperature gradient to form across the substrate through joule heating. The temperature difference ($\Delta T$) between the two NW electrode contacts was obtained by probing the variations ($\Delta R$) of the resistances, $R_n$ and $R_f$. It was found that the difference between $\Delta R_n$ and $\Delta R_f$ is proportional to $I_h^2$. The thermoelectric voltage ($\Delta V$), measured across the PbTe NW, increases linearly with increasing $I_h^2$ (not shown here). The thermoelectric power of the PbTe NW was obtained by the simple relation $S = \Delta V/\Delta T$, since it was confirmed that $\Delta V \propto I_h^2 \propto \Delta T$.

Figure 3(b) demonstrates the linearity of the thermoelectric voltage ($\Delta V$) measured with respect to the applied temperature difference ($\Delta T$), providing $S = -72\ \mu$V K$^{-1}$ at room temperature. The negative $S$ value indicates n-type carrier-dominated transport, which is consistent with the result of the FET device measurement. Other research groups

previously reported PbTe NW films with a positive $S$ value (p-type) [10–12]. In contrast, this is the first time that single n-type PbTe NWs with a negative $S$ value have been reported, which could be related to the Te-deficient composition of the NWs. It was reported that the $S$ value of n-type bulk PbTe is about $-300\ \mu V\ K^{-1}$ at the same carrier concentration [16]. The absolute $S$ value of the present NW is lower than that of bulk PbTe. Heremans *et al* showed the enhancement of the $S$ value of PbTe thin films with a grain size of 30–50 nm, which was attributed to an increase of the electron mean free path, resulting from the separation of higher energy electrons from lower energy electrons and the selective scattering of electrons or so-called electron energy filtering [17]. In order to explain unexpected lower $S$ value of the n-type PbTe NW, further details on thermoelectric properties including temperature-dependent thermal conductivity and thermoelectric power need to be investigated.

## 4. Conclusion

We synthesized single-crystalline PbTe NWs using a chemical vapor transport of $PbCl_2$ and Te powders. The PbTe NWs consisted of rock-salt structure PbTe nanocrystals uniformly grown in the [100] direction. Their average diameter is 130 nm. The NW FET devices were fabricated using an individual PbTe NW, showing its n-type semiconductor characteristics. The value of the mobility was determined to be about 0.83 $cm^2\ V^{-1}\ s^{-1}$, and the carrier concentration was estimated as $8.8 \times 10^{17}\ cm^{-3}$, by using the one-dimensional electrical transport model. Furthermore, these PbTe NWs exhibit the obvious n-type thermoelectric transport properties. The Seebeck coefficient of an individual PbTe NW was measured to be $S = -72\ \mu V\ K^{-1}$ at room temperature.

## Acknowledgments

This study was supported by KOSEF (R01-2008-000-10825-0; 2008-02364), KRF (2008-314-C00175), and MKE under the ITRC support program supervised by the IITA (2008-C1090-0804-0013). This research was also supported by a World Class University (WCU) program through the NRF funded by the Ministry of Education, Science and Technology (R31-10035). W Lee is grateful for the financial support of a grant from the 'Center for Nanostructured Materials Technology' under '21st Century Frontier R&D Programs' of the Ministry of Education, Science and Technology and KOSEF through National Core Research Center for Nanomedical Technology (R15-2004-024-00000-0). The SEM (Seoul), HVEM (Daejeon), XRD (Taegu), and XPS (Pusan) measurements were performed at the KBSI. The experiments at the PLS were partially supported by MOST and POSTECH.

## References

[1] Hu J, Odom T W and Lieber C M 1999 *Acc. Chem. Res.* **32** 435
Gudiksen M S, Lauhon L J, Wang J, Smith D C and Lieber C M 2002 *Nature* **415** 617
[2] Mokari T, Zhang M and Yang P 2007 *J. Am. Chem. Soc.* **129** 9864
[3] Urban J J, Talapin D V, Shevchenko E V and Murray C B 2006 *J. Am. Chem. Soc.* **128** 3248
[4] Wang W Z, Poudel B, Wang D Z and Ren Z F 2005 *Adv. Mater.* **17** 2110
[5] Qiu X F, Lou Y B, Samia A C S, Devadoss A, Burgess J D, Dayal S and Burda C 2005 *Angew. Chem. Int. Edn* **44** 5855
[6] Tong H, Zhu Y-J, Yang L X, Li L and Zhang L 2006 *Angew. Chem. Int. Edn* **45** 7739
[7] Li G-R, Yao C-Z, Lu X-H, Zheng F-L, Feng Z-P, Yu X-L, Su C-Y and Tong Y-X 2008 *Chem. Mater.* **20** 3306
[8] Zhang L, Yu J C, Mo M, Wu L, Kwong K W and Li Q 2005 *Small* **1** 349
[9] Fardy M, Hochbaum A I, Goldberger J, Zhang M M and Yang P 2007 *Adv. Mater.* **19** 3047
[10] Tai G, Zhou B and Guo W 2008 *J. Phys. Chem.* C **112** 11314
[11] Tai G, Guo W and Zhan Z 2008 *Cryst. Growth Des.* **8** 2906
[12] Yan Q, Chen H, Zhou W, Hng H H, Boey F Y C and Ma J 2008 *Chem. Mater.* **20** 6298
[13] Yang Y, Kung S C, Taggart D K, Xiang C, Yang F, Brown M A, Güell A G, Kruse T J, Hemminger J C and Penner R M 2008 *Nano Lett.* **8** 2447
[14] Liu W, Cai W and Yao L 2007 *Chem. Lett.* **36** 1362
[15] Goldberger J, Sirbuly D J, Law M and Yang P 2005 *J. Phys. Chem.* B **109** 9
[16] Harman T C, Spears D L and Manfra M J 1996 *J. Electron. Mater.* **25** 1121
Harman T C, Taylors P J, Spears D L and Walsh M P 2000 *J. Electron. Mater.* **29** L1
[17] Heremans J P, Thrush C M and Morelli D T 2004 *Phys. Rev.* B **70** 115334